Applied Geochemistry 151 (2023) 105627

Contents lists available at ScienceDirect

Applied Geochemistry

journal homepage: www.elsevier.com/locate/apgeochem

Identification of the sources of different phosphorus fractions in lake sediments by oxygen isotopic composition of phosphate

Zuxue Jin [a,b], Jingfu Wang [a,b,*], Ruixue Zhang [c], Peng Liao [a,b], Yong Liu [d], Jiaojiao Yang [a,b], Jingan Chen [a,b,**]

[a] State Key Laboratory of Environmental Geochemistry, Institute of Geochemistry, Chinese Academy of Sciences, Guiyang, 550081, PR China
[b] University of Chinese Academy of Sciences, Beijing, 100049, PR China
[c] College of Resource and Environmental Engineering, Guizhou University, Guiyang, 550025, PR China
[d] College of Biological and Environmental Engineering, Guiyang University, Guiyang, 550005, PR China

ARTICLE INFO

Editorial handling by: Dr Neus Otero

Keywords:
Phosphate
Oxygen isotopes
Source identification
Phosphorus fractions

ABSTRACT

Phosphorus (P) released from sediment driven by oxidation-reduction potential and enzymes can increase the concentrations of dissolved P in the overlying water, which trigger widespread algal blooms. Therefore, identification sediment P sources is critical for the management of P and restoration of eutrophic aquatic ecosystem. Sediment P fractions have been widely reported, whereas little is known regarding the source and pathway of different P fractions in eutrophic lake sediments. In this study, we applied chemical sequential extraction with oxygen isotopic compositions of phosphate ($\delta^{18}O_P$) to identify the inorganic P (P_i) source in the sediments of Lake Dianchi, China. Results show that contents of organic P (P_o), HCl-P_i, NaOH-P_i, and $NaHCO_3$-P_i of sediment were the main P fractions compared with that of sediment H_2O-P_i, which was attributed to the bioavailable difference of these P fractions. Significant difference on the equilibrium values of $\delta^{18}O_P$ ($\delta^{18}O_{P\text{-}eq}$), $\delta^{18}O_P$ of sediment P fractions, and $\delta^{18}O_P$ of external P was observed, which reflected the complex transformation processes of these P fractions in sediments. Further, the values of sediment $\delta^{18}O_{NaHCO3\text{-}Pi}$ at some sites (17.2–22.5‰) deviated from $\delta^{18}O_{P\text{-}eq}$ (14.7–19.0‰), and these values fell into the values of $\delta^{18}O_P$ for external P (7.7–23.8‰), suggesting that sediment $NaHCO_3$-P_i at these sites derived from external P. Comparison the values of sediment $\delta^{18}O_{NaOH\text{-}Pi}$ (14.5–24.9‰) with $\delta^{18}O_{P\text{-}eq}$ and $\delta^{18}O$ of external P sources suggested that sediment NaOH-P_i was not only from external P, but also from sedimentary P_o remineralization. P_i released from sediment NaOH-P_i may be responsible for the higher values of sediment $\delta^{18}O_{HCl\text{-}Pi}$ (15.2–20.8‰) than that of soils (13.1–15.3‰) and phosphate rock (8.9–12.6‰). Results gained from this study provided critical insights for the source and biogeochemical cycling of P across the sediment-water interface in the eutrophic lake.

1. Introduction

As the essential element of all livings, phosphorus (P) is one of the critically limited factors of water eutrophication. Excessive P discharged from both point and/or non-point sources into freshwater bodies could result in the water eutrophication (Lau and Lane, 2002; Kochian, 2012). Recent advances substantiated that in addition to external P, internal P released from sediments to overlying water can enhance the bioavailability and exchange of P at the sediment-water interface, which may potentially lead to extensive algal blooms (Zhu et al., 2013; Chen et al., 2016; Wang et al., 2016; Wu and Wang, 2017; Chen et al., 2019b). Orthophosphate (e.g., $H_2PO_4^-$, HPO_4^{2-}, and PO_4^{3-}) is a predominant and bioavailable form in sediments. Sediment inorganic P (P_i) sources include soils, phosphate fertilizers, domestic sewage, rock, and organic P (P_o) remineralization. Although sediment P_i fractions have been widely studied, the source and pathway of P_i fractions in sediments remain elusive.

Principles of mass balance and export coefficient models are

* Corresponding author. State Key Laboratory of Environmental Geochemistry, Institute of Geochemistry, Chinese Academy of Sciences, Guiyang, 550081, PR China.
** Corresponding author. State Key Laboratory of Environmental Geochemistry, Institute of Geochemistry, Chinese Academy of Sciences, Guiyang, 550081, PR China.
E-mail addresses: wangjingfu@vip.skleg.cn (J. Wang), chenjingan@vip.skleg.cn (J. Chen).

https://doi.org/10.1016/j.apgeochem.2023.105627
Received 26 August 2022; Received in revised form 2 March 2023; Accepted 7 March 2023
Available online 8 March 2023

traditional methods that have been used for identifying the P sources at watershed-scale (Dillon and Kirchner, 1975; Chen et al., 2019a; Rutledge and Chow-Fraser, 2019). While the mass balance method can not accurately identify the P export under similar land use in the watershed due to the distinct geology (Rutledge and Chow-Fraser, 2019), and the magnitude of nutrients exported from mixed, large agricultural watershed is difficult to evaluate, which may give rise to large uncertain results (Beaulac and Reckhow, 1982). Additionally, export coefficient models are very complicated that need extensive field investigations and simulation parameters (Chen et al., 2019a; Rutledge and Chow-Fraser, 2019). Further, extensive transformation of external P makes it more difficult to trace the sources of P in sediments. For example, soils, fertilizers, and domestic sewage could be transported into lake sediments (Wang et al., 2021). These particulate and dissolved P from external sources could be partially redistributed in sediments as iron (Fe) (hydr) oxides and authigenic minerals (Pistocchi et al., 2017; Yuan et al., 2019). Furthermore, P_i released from sedimentary P_o remineralization could also be redistributed in sediments P pools due to adsorption and precipitation (Joshi et al., 2015; Yuan et al., 2019; Wang et al., 2021). Such complex P transformation in sediments challenges the traditional methods to be a useful tool for the accurate identification of different P source. It is therefore of great importance to combine chemical sequential extraction with other advanced techniques to disclose the sources and associated with pathway processes of P fractions in sediments.

The oxygen isotopic compositions of phosphate ($\delta^{18}O_P$) is a state-of-the-art technology that can be regarded as a promising tool to track the biogeochemical cycling of P (Joshi et al., 2015; Granger et al., 2017; Zhao et al., 2021). Particularly, phosphate, Fe and Mn oxides, and water showed no exchange of oxygen during adsorption and desorption processes in the long term (Jaisi et al., 2010; Li et al., 2015). The oxygen of phosphate can be exchanged with oxygen from water via biological processes (e.g., enzymes and microorganisms). Regenerated P_i from orthophosphate monoesters (mono-P) and orthophosphate diesters (diester-P) during enzyme hydrolysis experiments demonstrated that the released P_i incorporated with one to two oxygen from water, resulting in distinctly lower signals of $\delta^{18}O_P$ than the equilibrium values of $\delta^{18}O_P$ ($\delta^{18}O_P$-eq) (Liang and Blake, 2006, 2009). In addition, the bacteria can significantly move the values of $\delta^{18}O_P$ in water towards $\delta^{18}O_{P\text{-}eq}$, resulting in obvious fractionations of $\delta^{18}O_P$ (Stout et al., 2014). With the improved theories for the fractionations in $\delta^{18}O_P$ associated with specific enzymes and microbials involved in P cycles (Liang and Blake., 2006, 2009), $\delta^{18}O_P$ has been gradually used as a tracer of P cycling in natural water and marine sediments (Joshi et al., 2015; Granger et al., 2017; Wei et al., 2021; Zhao et al., 2021). Such as, a recent study using $\delta^{18}O_P$ demonstrated that fertilizers and domestic sewage were the main P sources in the Huangbai River, China (Wei et al., 2021). Granger et al. (2017) reported that the distinct signals in $\delta^{18}O_P$ from the wastewater were lost within the river over a short distance due to rapid microbial cycling of P in the Upper River Taw catchment, UK. In addition, $\delta^{18}O_P$ demonstrated that P_o remineralization predominated P cycling in the Chesapeake Bay sediments (Joshi et al., 2015). It has been summarized that the specific $\delta^{18}O_P$ can be sourced from natural materials through previous published literatures that include domestic sewage (7.5‰–20‰), soils (5.0‰–25.0‰), sediments (7.5‰–25.0‰), fertilizers (12.5‰–25.0‰), and rock (0.0‰–20.0‰) from many regions (Tian et al., 2020). Moreover, these isotopic compositions of different sources in the same region have obvious difference (e.g., Wei et al., 2021). Specific $\delta^{18}O_P$ with varied P sources would be valuable to understand the transformation of sediment P under abiotic and biotic pathways.

The objectives of this study were to identify the source and pathway of different P fractions in sediments. To this end, we collected sediments from a eutrophic lake, Lake Dianchi historically suffered from both external P inputs and internal P release from sediments. Detailed objectives of this study were: (1) estimated P stocks in sediment and potential P sources and any differences among them; (2) characterized $\delta^{18}O_P$ of different sediment P_i fractions and potential P sources; (3) and assessed the possible sources of sediment different P_i fractions. Chemical sequential extraction is widely used to study P distributions in soils and sediments (Zhu et al., 2013; Helfenstein et al., 2018). $\delta^{18}O_P$, as an effective tracer, has been gradually applied to characterize P cycling in the Earth's environment (Joshi et al., 2015; Yuan et al., 2019; Zhao et al., 2021). Therefore, chemical sequential extraction and $\delta^{18}O_P$ were employed to address all three. Altogether, the new results gained from this study are important to advance our understanding of the fate and transport of P in lake sediments.

2. Materials and methods

2.1. Study sites

Lake Dianchi (102°36′-102°47′ E, 24°40′-25°02′ N), located in the Yunnan province, Southwest China, is the sixth largest freshwater lake in China. Lake Dianchi is seriously threatened by algal blooms (Jin et al., 2022). With the rapid urbanization of Kunming City in the 1980s, a large amount domestic sewage and agricultural runoff were discharged into the lake, resulting in the deterioration of water quality. In the 2000s, the water quality of Lake Dianchi was worse than class V (e.g., total P (TP) > 1.06 mg L^{-1}) (GB3838-2002), and became one of the most seriously polluted lakes in China (Li et al., 2007).

Sampling sites were showed in Fig. 1. Based on the report of Zhu et al. (2013), Site 1 is located in the north of the Lake Dianchi, near the algae accumulation region. The potential P source includes final effluent from wastewater treatment plant (WWTP) (13#). Site 2 is located in the northeast of the Lake Dianchi, near the flower planting region. The potential P source includes soils (flower planting region soils, 7#). Site 3 is located in the west of the Lake Dianchi, near the Mountain Guanyinshan phosphate rock region. The potential P source includes phosphate rock (12#). Site 4 is located in the east of the lake, near the Laoyu River watershed, where had been influenced agricultural runoff (phosphate fertilizer) and effluent from WWTP for a long time. The potential P source includes soils (forest soils, 8#), final effluent (14#), and phosphate fertilizers (16#). Site 5 is located in the southeast of Lake Dianchi, near the vegetable growing region. The potential P source includes soils (vegetable growing region soils) (9#). Site 6 is located in the south of the Lake Dianchi, near the Kunyang phosphate fertilizer factory. The potential P source includes soils (forest soils, 10#), phosphate rock (11#), and final effluent from WWTP (15#). Site 16 is located in the town/-township at Kunyang, Kunming City (three kinds of phosphate fertilizers were collected as for potential P sources). The flow direction of lake water is from north to south.

2.2. Sample collection

In April 2021, surface water, bottom water, surface sediments, and the samples of potential P sources were collected (Fig. 1). Sites 1 to 6, surface water and bottom water samples were collected using a stratified water sampler (WB-SS, Beijing Purity Instrument CO., LTD, China) from 0.5 m below the surface water and 0.5 m above sediments, respectively. Sediment samples were also collected using a Petersen grab sampler (PBS-411, Wuhan Petersen Technology CO., LTD, China) at the same sampling sites. Potential P sources' samples of Lake Dianchi watershed were also collected (sites 7–16), including soils, phosphate rock, effluent from WWTP, and phosphate fertilizers (three kinds of phosphate fertilizers came from Yunnan Phosphate Haikou CO., LTD, China, including KH_2PO_4, $NH_4H_2PO_4$, and $(NH_4)_2HPO_4$. Moreover, the raw materials of these fertilizers came from Haikou phosphate rock (see site 11#)). Water samples were stored in high density polyethylene bottles. Soils, fertilizers, and sediments were stored in centrifuge tubes (50 mL, Corning, Germany). Porewater samples were prepared by centrifuging the sediment samples (at 4390 g for 15 min). All samples were stored in ice boxes and transported to the laboratory for analysis.

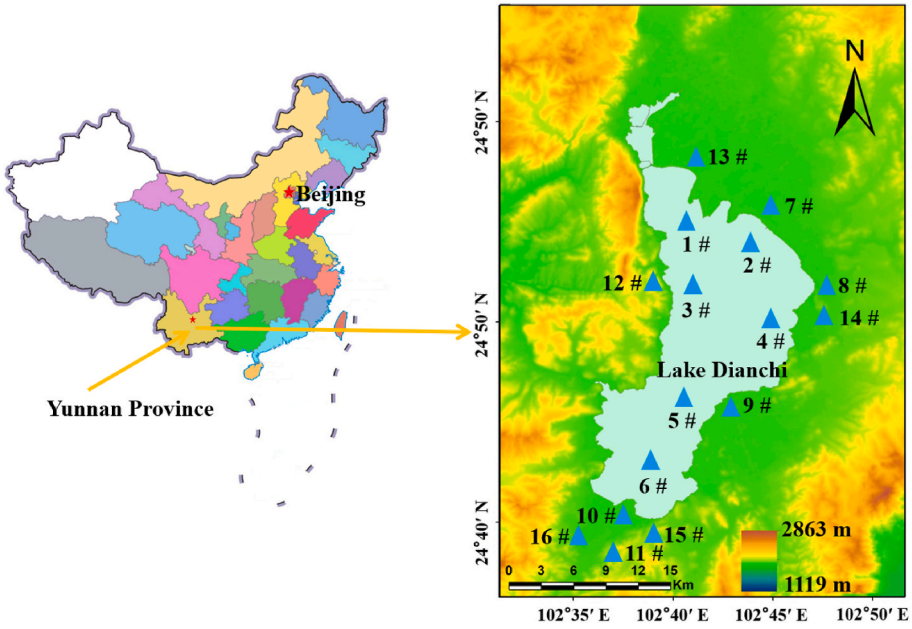

Fig. 1. Map of sampling sites.

2.3. Analysis of P contents in sediments and soils, and P concentrations in water samples

Sediment and soil samples were freeze-dried and then were ground and sieved through a 200-mesh sieve and stored at −20 °C before analysis. TP in soils and sediments were determined by the $HClO_4$–H_2SO_4 digestion method (Frankowski et al., 2002). P fractions of soils and sediments were determined based on the modification Hedley (Hedley et al., 1982) method and as described in Tian et al. (2020). Briefly, Milli-Q water, 0.5 M $NaHCO_3$ (pH = 8.5), 0.1 M NaOH, and 1 M HCl solutions (solid:liquid = 1:60) were used to extract H_2O-P_i, $NaHCO_3$-P_i, NaOH-P_i, and HCl-P_i, respectively. All extraction solutions were then centrifuged (at 4390 g for 15 min) and filtered through 0.45 μm filters (TJMF50, Tianjin Jinteng Experimental Equipment CO., LTD, China). Contents of P_i (i.e., H_2O-P_i, $NaHCO_3$-P_i, NaOH-P_i, and HCl-P_i) were measured using the molybdenum blue method (Murphy and Riley, 1962). P_o in soils and sediments was calculated by the difference between TP and P_i (Tang et al., 2018).

Water samples were filtered through 0.45 μm filters for analysis P concentrations. Subsequently, dissolved P_i concentrations of water samples were measured by using the molybdenum blue method (Murphy and Riley, 1962), total dissolved P concentrations were digested by potassium persulfate and then measured by using the molybdenum blue method. All samples were measured at least in triplicate.

2.4. Analysis the oxygen isotopes of phosphate and water

The pretreatment of $\delta^{18}O_P$ in effluent was based on the method recommended by McLaughlin et al. (2004). No $\delta^{18}O_P$ from lake water samples were obtained due to the low concentration of dissolved P_i (<0.01 mg L^{-1}) in the water column, although these data were helpful to elucidate the P cycling at the sediment-water interface. The pretreatment of $\delta^{18}O_P$ in various P_i fractions in sediments (sites 1–6), soils, and phosphate rock were performed with reference to the method proposed by Liu et al. (2019). All acquired Ag_3PO_4 samples were freeze-dried and all samples were thoroughly homogenized and loaded into quartz tubes. The quartz tubes were pumped to vacuum and sealed, and then were heated at ~550 °C for 3 min to remove residual organic matter and water (Blake et al., 2005; Sandy et al., 2013; Jaisi and Blake, 2014). Then Ag_3PO_4 solid was stored in 1.5 mL centrifuge tubes and placed in the dark. Subsequently, the Ag_3PO_4 solid was examined by scanning electron microscopy (SEM, JSM−6460LV, Japan) and X-ray diffraction (XRD, Empyrean, PANalytical B.V., Holland) at the Institute of Geochemistry, Chinese Academy of Sciences (details can be found in Text S1 and Fig. S1).

Approximately 0.5 mg Ag_3PO_4 was weighed and placed in a silver cup, the cups were tightly folded to minimize the amount of trapped air. Ag_3PO_4 was tested using a high temperature (1380 °C) pyrolysis stable isotope ratio mass spectrometer (HT−IRMS, Flash EA 1112, Mat 253, Thermo Co, Ltd) at the Isotopic Laboratory of the Third Institute of Oceanography, the Ministry of Natural Resources, China. The oxygen yield of Ag_3PO_4 after pyrolysis was calculated and with >90% yield was considered acceptable. $\delta^{18}O_p$ was calibrated using two oxygen isotope reference materials: Benzoic acid (IAEA-601, 23.3 ± 0.3‰) and silver phosphate (Ag_3PO_4, 21.7 ± 0.3‰, B2207, Elemental Microanalysis, UK). Values of $\delta^{18}O_p$ have an analytical precision of ±0.3‰. All values of $\delta^{18}O_p$ are reported with respect to the Vienna Standard Mean Ocean Water (VSMOW), calculated as:

$$\delta^{18}O(‰) = \left[\frac{R\left({}^{18}O/{}^{16}O_{sample}\right)}{R\left({}^{18}O/{}^{16}O_{VAMOW}\right)} - 1\right] \times 1000 \quad (1)$$

Where R ($^{18}O/^{16}O$) represents the oxygen isotope abundance ratio.

The oxygen isotopic values in surface water, bottom water, and porewater were measured by using an LGR Isotopic Water Analyzer (DLT-100, Los Gatos Research Co, USA) (detailed by Table S1).

2.5. Calculation of phosphate oxygen isotopic equilibrium values

The values of $\delta^{18}O_{p\text{-}eq}$ are widely selected as a reference for tracing P cycling processes (Pistocchi et al., 2017; Zhao et al., 2021), which was calculated using the empirical equation modified by Chang and Blake (2015):

$$\delta^{18}O_{p-equ} = \left(\delta^{18}O_w + 1000\right) \times \exp\left(\left(14.43 \times 1000 / T - 26.54\right) / 1000\right) - 1000 \quad (2)$$

where T is temperature (K), $\delta^{18}O_w$ represent the oxygen isotopic values in water (including surface water, bottom water, and porewater) (Table S1).

2.6. Calculation of phosphate oxygen isotopic values for inorganic phosphate regenerated from organic phosphorus

According to Joshi et al. (2015) description (see results and discussion, isotopic composition of sediment P pool, Joshi et al., 2015), the bulk of P_o is formed in spring-early summer months and the temperature and in equilibrium with measured surface water ($\delta^{18}O_W$ values of −4.83 to −4.60‰) inside cells as per Chang and Blake (2015). The values of $\delta^{18}O_{po}$ can be calculated by using equation (2). The range of $\delta^{18}O_P$ values of regenerated P_i from mono-P and diester-P can be calculated using equations of Table 1 (Liang and Blake., 2006, 2009).

3. Results and discussion

3.1. Contents/concentrations of sediment and potential P sources

In descending order of content, the P fractions in sediments were P_o (699 ± 53 mg kg^{-1}) > HCl-P_i (683 ± 156 mg kg^{-1}) > NaOH-P_i (566 ± 275 mg kg^{-1}) > $NaHCO_3$-P_i (123 ± 67 mg kg^{-1}) > H_2O-P_i (3 ± 0 mg kg^{-1}) (Fig. 2). Contents of H_2O-P_i were very small and contributed 0.2% of TP (Fig. S2), consequently, the roles of H_2O-P_i in overall P cycling are considered as negligible. Such variation on sediment P fractions was essentially attributed to their bio-available difference (Zhu et al., 2013). P_o was the predominant P fractions. So high contents of P_o reflected that sediment could contain plenty of plant debris (e.g., algae) (Xie et al., 2019; Jin et al., 2022). Solution ^{31}P NMR demonstrated that P_o is composed of mono-P and diester-P (Table S2). No drastic changes were found in the sediment P_o contents from all sample sites (Fig. 2e), suggesting that the effect of three points discharge from WWTP on this P fraction in the sediments was insignificant. This view was further supported by the negligible difference on the concentrations of dissolved P_i and total dissolved P (TDP) in effluent from three WWPTs (Table S3), which suggested that the more than 95% TDP was in the form of dissolved P_i.

Substantial difference on contents of sediment HCl-P_i was observed (Fig. 2d). Such as, contents of HCl-P_i at site 6 were the highest (954 ± 12 mg kg^{-1}) compared with contents of HCl-P_i in the rest sites. In addition, essentially higher content of HCl-P_i in site 6 than that of its one potential P source (265 ± 5 mg kg^{-1}, 10#, Table S3) was also observed, suggesting that high content likely resulted from the phosphate rock (He et al., 2015). Further, phosphate rock (site 11) contains abundant phosphate (P_2O_5, Table S4). The second most abundant sediment HCl-P_i at site 2 was likely driven by water and soil loss (Fig. 2d). This point was further supported by similar contents of HCl-P_i between sediment at site 2 (759 ± 22 mg kg^{-1}, Fig. 2) and corresponding soil at site 7 (718 ± 29 mg kg^{-1}, Table S3).

Table 1
The values of $\delta^{18}O$ in regenerated P_i from organic P remineralization.

P_o	Enzyme	F (‰)	$\delta^{18}O_p$ of regenerated P_i
Mono-P	APase	−26	$0.25*(\delta^{18}O_w + F_{APase}) + 0.75*\delta^{18}O_{Po}$
	5′Nase	−10	$0.25*(\delta^{18}O_w + F_{5'Nase}) + 0.75*\delta^{18}O_{Po}$
RNA	PDase	+20	$0.25*(\delta^{18}O_w + F_{PDase}) + 0.25*(\delta^{18}O_w + F_{APase}) + 0.5*\delta^{18}O_{Po}$
	APase	−30	
	PDase	+20	$0.25*(\delta^{18}O_w + F_{PDase}) + 0.25*(\delta^{18}O_w + F_{5'Nase}) + 0.5*\delta^{18}O_{Po}$
	5′Nase	−10	
DNA	PDase	−20	$0.25*(\delta^{18}O_w + F_{PDase}) + 0.25*(\delta^{18}O_w + F_{APase}) + 0.5*\delta^{18}O_{Po}$
	APase	−30	
	PDase	−20	$0.25*(\delta^{18}O_w + F_{PDase}) + 0.25*(\delta^{18}O_w + F_{5'Nase}) + 0.5*\delta^{18}O_{Po}$
	5′Nase	−10	

Note: P_o, organic P; Mono-P, phosphomonoesters; APase, alkaline phosphatase; 5′Nase, 5′-nucleotidase; PDase, phosphodiesterase; F, factors. Data from Liang and Blake (2006, 2009).

The consistent changes of contents of NaOH-P_i and $NaHCO_3$-P_i in sediments from all sample sites were observed (Fig. 2b and c), which possibly reflected the same site with the similar P sources. Particularly, contents of NaOH-P_i and $NaHCO_3$-P_i at site 4 were fundamentally higher than that of the rest sites (Fig. 2 b, c), which demonstrated that site 4 received more P sources than others. This result was further demonstrated by previous a study, which suggested that sites 4 has been received wastewater from Chengong district of Kunming city and agricultural runoff (phosphate fertilizers) for a long time (Song et al., 2019). Moreover, the dissolved P_i concentration of effluent (site 14, Table S3) was significantly higher than that of the lake water (site 4, Table S3) over a short distance (approximately ~3 km), which suggested that dissolved P_i from effluent was likely absorbed by suspended particles. Previous studies also demonstrated that contents P_i of suspended particles were higher than that of sediments in Lake Dianchi (Xie et al., 2019; Jin et al., 2022). These factors may explain why the highest contents of NaOH-P_i and $NaHCO_3$-P_i in sediments at site 4 than that of others were observed after these suspended particles sedimentation. The long-term effects of dissolved P_i from wastewater and agricultural runoff on P fractions of sediment column over the past several decades warrant further study.

3.2. The difference on $\delta^{18}O_P$ of sediment P_i fractions and potential P sources

Significant difference on $\delta^{18}O_P$ of different P_i fraction in sediments and potential P sources was observed from all samples (Fig. 3). These values of $\delta^{18}O_P$ in three different P_i fraction of sediments were either close to $\delta^{18}O_{P\text{-}eq}$ or deviated from $\delta^{18}O_{P\text{-}eq}$. Such difference reflected complex biogeochemical cycling of these P_i fractions, particularly for these isotopic signals towards $\delta^{18}O_{P\text{-}eq}$ (see 3.3).

Same P_i fraction of soils have obviously different values of $\delta^{18}O_P$ (Fig. 3), which could be driven by divergent equilibrium conditions (soil temperature and $\delta^{18}O_{H2O}$), varied P sources, and biological processes (Lei et al., 2019; Wells et al., 2022). Firstly, short-term diurnal changes in soil temperature and $\delta^{18}O_{H2O}$ have little effect on contents of soil P_i fractions and their corresponding $\delta^{18}O_P$ (Lei et al., 2019). This suggests that current $\delta^{18}O_P$ of soil P_i fractions likely resulted from long-term influence of above-mentioned factors. Secondly, soils receive PO_4^{3-}. Phosphate fertilizer and manure are excluded here because of higher $\delta^{18}O_P$ of soil P_i fractions than $\delta^{18}O_{Phosphate\ fertilizer}$ (Fig. 3) and $\delta^{18}O_P$ of manure (13.5‰) (Granger et al., 2017). While plant leaves have $\delta^{18}O_P$ up to ~30‰ (Pfahler et al., 2013), and that thus is a potential P source for soil. Moreover, enzyme(s) and microorganisms can also shift the $\delta^{18}O_P$ of soil P_i fractions. Liang and Blake. (2006, 2009) charactered $\delta^{18}O_P$ from P_o remineralization, demonstrating that the $\delta^{18}O_P$ of regenerated P_i were obviously lower than the $\delta^{18}O_{P\text{-}eq}$. In contrast, the $\delta^{18}O_P$ of labile P_i fractions (e.g., $NaHCO_3$-P_i) could shift towards $\delta^{18}O_{P\text{-}eq}$ driven by microorganisms (Jaisi et al., 2011; Wells et al., 2022). More works are required to reveal the effect of each factor to the $\delta^{18}O_P$ of soil P_i fractions.

Effluent from WWPTs have obviously different values of $\delta^{18}O_P$ (Fig. 3), which was likely attributed to different wastewater sources (e.g., agricultural, industrial, and domestic). Similar results of effluents from two WWTPs in the Upper River Taw catchment with different values of $\delta^{18}O_P$ were also observed by Granger et al. (2017), which demonstrated that the mean value of $\delta^{18}O_P$ from WWTP1 (19.2‰) was higher than that of WWTP2 (16.7‰). Significantly decreased concentrations of dissolved P_i from WWTP (>0.06 mg L^{-1}) to the lake (<0.01 mg L^{-1}) (Table S3) resulted in no available $\delta^{18}O_P$ values of dissolved P_i from lake water in this study, although these were helpful for the explanation of $\delta^{18}O_P$ from sediment P_i fractions. Similar results were observed in the beult catchment in England, with a substantial decrease in dissolved P_i concentrations downstream of a WWTP but with little shift in $\delta^{18}O_P$ values (Gooddy et al., 2016). Furthermore, in another

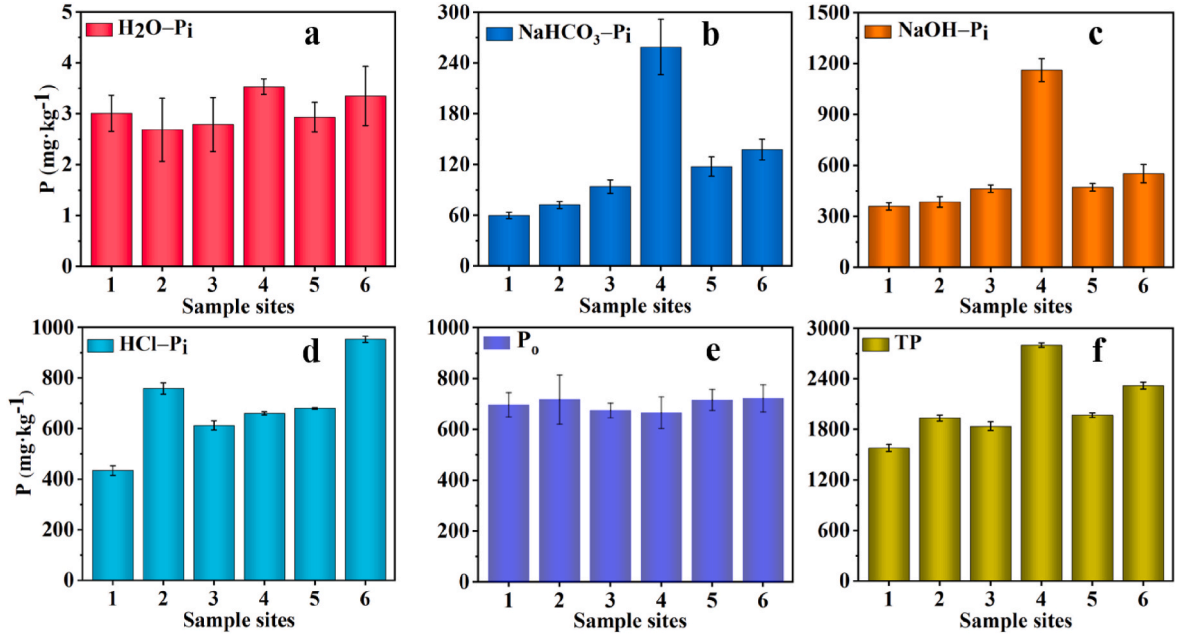

Fig. 2. Contents of different P fractions in sediments. Panel a, b, c, d, e, and f represent H_2O-P_i, $NaHCO_3$-P_i, NaOH-P_i, HCl-P_i, P_o, and TP, respectively. Error bar represents standard deviations of triplicated measurements.

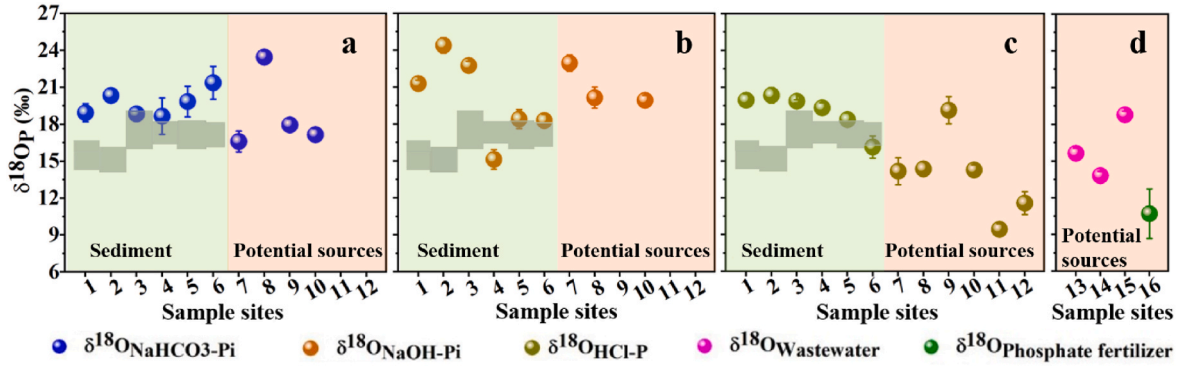

Fig. 3. The values of $\delta^{18}O_P$ for different P fractions in sediments (sites 1−6) and potential P (sites 7−16). The gray box line region represents the $\delta^{18}O_{P\text{-}eq}$ values calculated using season-average temperature data (11–23 °C) at sediment-water interface and measured the values of $\delta^{18}O_{porewater}$ (−8.07~-6.02‰) (Table S1) in April 2021. Note: Panel a, b, and c represent the values of $\delta^{18}O_{NaHCO3\text{-}Pi}$, $\delta^{18}O_{NaOH\text{-}Pi}$, and $\delta^{18}O_{HCl\text{-}Pi}$ in sediment and potential sources, respectively. Panel d represents the values of $\delta^{18}O_{wastewater}$ and $\delta^{18}O_{Phosphate\ fertilizer}$. The values in $\delta^{18}O_{NaHCO3\text{-}Pi}$ and $\delta^{18}O_{NaOH\text{-}Pi}$ of phosphate rock at site 11–12, and the value in $\delta^{18}O_{NaOH\text{-}Pi}$ of soil at site 9 were missing. Error bar represents the standard deviations of at least duplicate measurements. Where error bars are not visible, they are smaller than the data symbols.

study, repetitive samples from effluent of WWTPs for three sites were collected over 8–24 h, suggesting that varied phosphate concentrations but negligible differences of $\delta^{18}O_P$ were observed; additionally, $\delta^{18}O_P$ from downstream river to a distance of at least 3 km reflected their mixed P sources from WWPT and upstream river (Gooddy et al., 2018). Accordingly, more evidence is required to reveal the $\delta^{18}O_P$ variations along the same reach in Lake Dianchi catchment in our ongoing work.

3.3. Indication of sediment P_i sources

To further elucidate the P sources of sediment P_i fractions, analyzing $\delta^{18}O_P$ of sediment P_i fractions and potential P sources allowed differentiating P fluxes driven by abiotic and biotic pathways. Drastic contents of different P_i fractions from sediments were observed (e.g., $NaHCO_3$-P_i and NaOH-P_i of sediments at site 4, HCl-P_i of sediments at site 6) (Fig. 2b, c, d), such difference reflected that at these sites were probably received more P sources. Combing these sediment P contents with their corresponding $\delta^{18}O_P$ and $\delta^{18}O_P$ of potential P sources demonstrated that site 4 might be received more effluent from WWTP, site 6 received more phosphate rock (Figs. 2–3). These results are consistent with previous studies, which suggested that the east (site 4) and south (site 6) of the lake had influenced by their corresponding external P over the past several decades (He et al., 2015; Song et al., 2019). The values of $\delta^{18}O_{NaOH\text{-}Pi}$ and the values of $\delta^{18}O_{NaHCO3\text{-}Pi}$ in sediments at some sites (e.g., sites 1–2, Fig. 3a and b) obviously deviated from the values of $\delta^{18}O_{p\text{-}eq}$ and fell into the ranges of $\delta^{18}O_P$ from corresponding P_i fractions of soils, indicating that sediment NaOH-P_i and $NaHCO_3$-P_i at these sites may be derived from soils. This conclusion was further supported by previous a study, indicating that soil erosion rates averaged 2133 t km^{-2} yr^{-1} in Lake Dianchi watershed estimated by ^{137}Cs (Niu et al., 2015). Nevertheless, no information is available about the residence time of sediment and P turnover rates in the lake. We cannot entirely demonstrate that these isotopic values of sediment P_i fractions are simply source-inherited isotopic signals. More direct evidence for the residence time of sediment and P turnover rates are needed to decide all two. The value of $\delta^{18}O_{NaOH\text{-}Pi}$ for site 2 (24.4 ± 0.5‰) was

higher than that of potential P sources (≤23.8‰) (Fig. 3), which is suggestive of unknown P sources.

P_i released from sediment P_o remineralization may be an important P source for sediment NaOH-P_i. Sediment NaOH-P_i has a high degree of bioavailability, and P from multiple sources (e.g., effluent, phosphate fertilizers, soils, and P_o remineralization) could be closely associated with Fe and Al (hydr)oxides (Jaisi and Blake, 2014; Wang et al., 2021). Typically, the values of $\delta^{18}O_{NaOH\text{-}Pi}$ in sediments overlap or approach to the $\delta^{18}O_{p\text{-}eq}$ (Joshi et al., 2016; Lei et al., 2019; Liu et al., 2019). The values of $\delta^{18}O_{NaOH\text{-}Pi}$ (18.4 ± 0.5‰) in sediments at sites 5–6 were closed to the $\delta^{18}O_{p\text{-}eq}$ (16.1–18.2‰) (Fig. 3b), suggesting that sediment NaOH-P_i has been undergone biological modification (Yuan et al., 2019). It has been showed that isotopic signals of $\delta^{18}O_P$ can shift towards $\delta^{18}O_{p\text{-}eq}$ driven by microorganisms (Jaisi et al., 2011; Stout et al., 2014; Granger et al., 2017). Alternatively, the values of $\delta^{18}O_{NaOH\text{-}Pi}$ in sediments at sites 5–6 were slightly lower than that of potential P sources (≥18.8‰, $\delta^{18}O_{NaOH\text{-}Pi}$ in soils at sites 10 and $\delta^{18}O_P$ in effluent at site 15, Fig. 3b), which suggested that lake sediments at sites 5–6 have been received another negatively isotopic signal P source besides soils and effluent. This view can be further supported by following statement. The values of $\delta^{18}O_w$ ranged from −4.83‰ to −4.60‰ in surface water (Table S1) with surface temperature of 18–23 °C, according to equation (2), the values of $\delta^{18}O_{Po}$ ranged from 17.5‰ to 18.5‰. The values in $\delta^{18}O_P$ of regenerated P_i from P_o were ranged from −6.2‰ to 10.3‰ according to the equations of Table 1. The calculated values of $\delta^{18}O_P$ (≤10.3‰) were lower than the values of sediment $\delta^{18}O_{NaOH\text{-}Pi}$ for sites 5–6 (18.4 ± 0.5‰). In addition, obvious negative correlation was found between sediment P_o/TP and sediment NaOH-P_i/TP ($r = -0.66$, $P < 0.01$, Fig. 4a). These observations suggested that P_i released from sedimentary P_o (compositions of P_o in sediment, Table S2) remineralization may be a source for sediment NaOH-P_i. Taken together, we consider the most likely interpretation for the values of $\delta^{18}O_{NaOH\text{-}Pi}$ in sediments at sites 5–6 and relatively higher P contents than that of the rest sites except site 4 to be tighter P_o remineralization. Among other things, more observational evidence of sedimentary P_o remineralization and targeted studies of their effects on sediment P_i redistribution are needed to further reveal P cycling at sediment-water interface.

P_i released from redox sensitive P fraction may be responsible for the higher values of sediment $\delta^{18}O_{HCl\text{-}Pi}$ than that of corresponding P sources. The values of sediment $\delta^{18}O_{HCl\text{-}Pi}$ (15.2–20.8‰) were higher than the values of soil $\delta^{18}O_{HCl\text{-}Pi}$ (13.1–15.3‰, except site 9 (18.0–20.2‰)) and phosphate rock (8.9–12.6‰), and lower than that of sediment NaOH-P_i (17.7–24.9‰, except site 4 (14.5–16.0‰)) (Fig. 3c). These $\delta^{18}O_P$ results suggested that P_i released from sediment NaOH-P_i was a P source for sediment HCl-P_i besides soil and phosphate rock. As expected, sediment P_i extracted by NaOH can be associated with Fe and Al oxides or hydroxides, thus the Fe oxides-bound phosphate has generally been considered as redox sensitive fraction. Previous a study also demonstrated that Fe-redox state controlled the concentration of P_i in sediment porewater in the same study area of Lake Dianchi (Wu and Wang, 2017) and therefore authigenic apatite could generate when the concentration of P_i in porewater was supersaturation (van Cappellen and Berner., 1991; Li et al., 2015; Joshi et al., 2015; Zhao et al., 2021). This conclusion was also further supported by a significant negative correlation between sediment HCl-P_i/TP and sediment NaOH-P_i/TP ($r = -0.92$, $P < 0.01$, Fig. 4b) and an obvious positive correlation between sediment $\delta^{18}O_{NaOH\text{-}Pi}$ and sediment $\delta^{18}O_{HCl\text{-}Pi}$ ($r = 0.63$, $P < 0.01$, Fig. S3a). Alternatively, the P_i released from sedimentary P_o remineralization diffused into porewater, which also induced the precipitation of authigenic apatite due to supersaturation of porewater P_i. However, the observed a weak negative correlation between the values of sediment $\delta^{18}O_{HCl\text{-}Pi}$ and the values of $\delta^{18}O_{water}$ ($r = -0.36$, $P < 0.01$, Fig. S3b), and the observed a weak positive correlation between the values of sediment $\delta^{18}O_{HCl\text{-}Pi}$ and sediment P_o/TP ($r = 0.46$, $P < 0.01$, Fig. S3c) suggested that P_i released from sedimentary P_o remineralization might be an insignificant source for sediment HCl-P_i. Instead, P_i released from sedimentary P_o remineralization was an important P source for sediment HCl-P_i and thus the values of $\delta^{18}O_{HCl\text{-}Pi}$ should be lower than that of soils and rocks due to low values of $\delta^{18}O$ in regenerated P_i from sedimentary P_o remineralization (≤10.3‰). However, sediment HCl-P_i may include authigenic P and detrital P (Ruttenberg, 1992; Yuan et al., 2019) and corresponding values of $\delta^{18}O$ in sediment HCl-P_i reflect their mixed isotopic signals. More direct evidences are needed to reveal the stocks and $\delta^{18}O$ of authigenic P and detrital P in sediment in ongoing work.

4. Conclusion

Combing chemical sequential extraction with $\delta^{18}O_P$ can improve the biogeochemical cycling information of sediment P fractions. Results showed that sediment P_i fractions and potential P sources (e.g., soils, phosphate fertilizers, phosphate rock, and effluent) have obviously different values of $\delta^{18}O_P$, which was helpful to identify biogeochemical cycling of P. Sediment P_i fractions are not only from external P, but also from transformation of sediment P fractions. Potential P sources (e.g., effluent, phosphate fertilizers, and phosphate rock) could be redistributed in sediment P_i fractions (e.g., $NaHCO_3$-P_i, NaOH-P_i, and HCl-P_i). P_i released from sedimentary P_o remineralization may be a source for sediment NaOH-P_i. P_i released from sediment NaOH-P_i may be responsible for the higher values of sediment $\delta^{18}O_{HCl\text{-}Pi}$ than that of potential P sources. Collectively, our study highlighted that $\delta^{18}O_P$ can provide direct evidence for the source tracing of sediment P. These results supplemented the current database on the values of $\delta^{18}O_P$ for various P sources and sediment P_i fractions, particularly in freshwater ecosystem, which improved our current understanding of sediment P cycling and lake nutrient management.

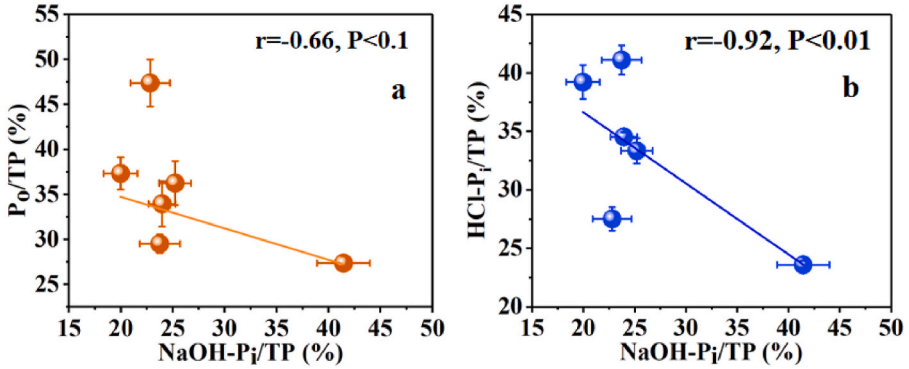

Fig. 4. The correlation of sediment P_o/TP and sediment NaOH-P_i/TP (panel a), and sediment HCl-P_i/TP and sediment NaOH-P_i/TP (panel b).

Declaration of competing interest

The authors declare that they have no known competing financial interests or personal relationships that could have appeared to influence the work reported in this paper.

Data availability

No data was used for the research described in the article.

Acknowledgements

This study was sponsored jointly by the Strategic Priority Research Program of CAS (No. XDB40020400), the National Key R&D Plan of China (2021YFC3201000), the Science and Technology Service Plan of CAS (KFJSTSQYZD202124001), the Central Leading Local Science and Technology Development Fund Project (20214028), the Chinese NSF Project (No. 41773145, 41977296, 41907279), the Youth Innovation Promotion Association CAS (No. 2019389), and the CAS Interdisciplinary Innovation Team. The authors would like to acknowledge Jianyang Guo for him continued support and critical feedback to this manuscript.

Appendix A. Supplementary data

Supplementary data to this article can be found online at https://doi.org/10.1016/j.apgeochem.2023.105627.

References

Beaulac, M.N., Reckhow, K.H., 1982. An examination of land use – nutrient export relationships. J. Am. Water Resour. Assoc. 18 (6), 1013–1024. https://doi/10.1111/j.1752-1688.1982.tb00109.x.

Blake, R., O'Neil, J.R., Surkov, A.V., 2005. Biogeochemical cycling of phosphorus: insights from oxygen isotope effects of phosphoenzymes. Am. J. Sci. 305, 596–620. https://doi.org/10.2475/ajs.305.6-8.596.

Chang, S.J., Blake, R.E., 2015. Precise calibration of equilibrium oxygen isotope fractionations between dissolved phosphate and water from 3 to 37 °C. Geochem. Cosmochim. Acta 150, 314–329. https://doi.org/10.1016/j.gca.2014.10.030.

Chen, M.S., Ding, S.M., Liu, L., Xu, D., Gong, M.D., Tang, H., Zhang, C.S., 2016. Kinetics of phosphorus release from sediments and its relationship with iron speciation influenced by the mussel (*Corbicula fluminea*) bioturbation. Sci. Total Environ. 542, 833–840. https://doi.org/10.1016/j.scitotenv.2015.10.155.

Chen, J., Xu, H., Zhan, X., Zhu, G.W., Qin, B.Q., Zhang, Y.L., 2019a. Mechanisms and research methods of phosphorus migration and transformation across sediment-water interface. J. Lake Sci. 31 (4), 907–918. https://doi.org/10.18307/2019.0416 (In Chinese).

Chen, Q., Chen, J.A., Wang, J.F., Guo, J.Y., Jin, Z.X., Yu, P.P., Ma, Z.Z., 2019b. In situ, high-resolution evidence of phosphorus release from sediments controlled by the reductive dissolution of iron-bound phosphorus in a deep reservoir, southwestern China. Sci. Total Environ. 666, 39–45. https://doi.org/10.1016/j.scitotenv.2019.02.194.

Dillon, P.J., Kirchner, W.B., 1975. Effects of geology and land-use on export of phosphorus from watersheds. Water Res. 9, 135. https://doi.org/10.1016/0043-1354(75)90002-0.

Frankowski, L., Bolaiek, J., Szostek, A., 2002. Phosphorus in bottom sediments of pomeranian bay (Southern Baltic-Poland). Estuar. Coast Shelf Sci. 54, 1027–1038. https://doi.org/10.1006/ecss.2001.0874.

GB3838−2002, 2002. China's National Standard "Environmental Quality Standards for Surface Water", Ministry of Environmental Protection of the People's Republic of China and General Administration of Quality Supervision. Inspection and Quarantine of the People's Republic of China.

Gooddy, D.C., Bowes, M.J., Lapworth, D.J., Lamb, A.L., Williams, P.J., Newton, R.J., Davies, C.L., Surridge, B.W.J., 2018. Evaluating the stable isotopic compositions of phosphate as a tracer of phosphorus from waste water treatment works. Appl. Geochem. 95, 139–146. https://doi.org/10.1016/j.apgeochem.2018.05.025.

Gooddy, D.C., Lapworth, D.J., Bennett, S.A., Heaton, T.H.E., Williams, P.J., Surridge, B. W.J., 2016. A multi-stable isotope framework to understand eutrophication in aquatic ecosystems. Water Res. 88, 623–633. https://doi.org/10.1016/j.watres.2015.10.046.

Granger, S.J., Heaton, T.H.E., Pfahler, V., Blackwell, M.S.A., Yuan, H.M., Collins, A.L., Gan, J., 2017. The oxygen isotopic composition of phosphate in river water and its potential sources in the upper river Taw catchment, UK. Sci. Total Environ. 574, 680–690. https://doi.org/10.1016/j.scitotenv.2016.09.007.

He, J., Chen, C.Y., Deng, W.M., Xu, X.M., Wang, S.R., Liu, W.B., Wu, X., Li, W., 2015. Distribution and release characteristics of phosphorus in water-sediment interface of Lake Dianchi. J. Lake Sci. 27 (5), 799–810. https://doi.org/10.18307/2015.0506 (In Chinese).

Hedley, M.J., Stewart, J.W.B., Chauhan, B.S., 1982. Changes in inorganic and organic soil phosphorus fractions induced by laboratory incubations. Soil Sci. Soc. Am. J. 46, 970–976. https://doi.org/10.2136/sssaj1982.03615995004600050017x.

Helfenstein, J., Tamburini, F., von Sperber, C., Massey, M.S., Pistocchi, C., Chadwick, O. A., Vitousek, P.M., Kretzschmar, R., Frossard, E., 2018. Combing spectroscopic and isotopic techniques gives a dynamic view of phosphorus cycling in soil. Nat. Commun. 9, 3226. https://doi.org/10.1038/s41467-018-05731-2.

Jaisi, D.P., Blake, R.E., 2014. Advances in using oxygen isotope ratios of phosphate to understand phosphorus cycling in the environment. Adv. Agron. 125, 1–54. https://doi.org/10.1016/B978-0-12-800137-0.00001-7.

Jaisi, D.P., Blake, R.E., Kukkadapu, R.K., 2010. Fractionation of oxygen isotopes in phosphate during its interactions with iron oxides. Geochem. Cosmochim. Acta 74, 1309–1319. https://doi.org/10.1016/j.gca.2009.11.010.

Jaisi, D.P., Kukkadapu, R.K., Stout, L.M., Varga, T., Blake, R.E., 2011. Biotic and abiotic pathways of phosphorus cycling in minerals and sediments: insights from oxygen isotope ratios in phosphate. Environ. Sci. Technol. 45, 6254–6261. https://doi.org/10.1021/es200456e.

Jin, Z.X., Wang, J.F., Jiang, S.H., Yang, J.J., Qiu, S.R., Chen, J.A., 2022. Fuel from within: can suspended phosphorus maintain algal blooms in Lake Dianchi. Environ. Pollut. 311, 119964 https://doi.org/10.1016/j.envpol.2022.119964.

Joshi, S.R., Kukkadapu, R.K., Burdige, D.J., Bowden, M.E., Sparks, D.L., Jaisi, D.P., 2015. Organic matter remineralization predominates phosphorus cycling in the mid-bay sediments in the Chesapeake Bay. Environ. Sci. Technol. 49, 5887–5896. https://doi.org/10.1021/es5059617.

Joshi, S.R., Li, X.N., Jaisi, D.P., 2016. Transformation of phosphorus pools in an agricultural soil: an application of oxygen-18 labeling in phosphate. Soil Sci. Soc. Am. J. 80, 69–78. https://doi.org/10.2136/sssaj2015.06.0219.

Kochian, L.V., 2012. Rooting for more phosphorus. Nature 488, 466–467. https://doi.org/10.1038/488466a.

Lau, S.S., Lane, S.N., 2002. Biological and chemical factors influencing shallow lake eutrophication: a long-term study. Sci. Total Environ. 288, 167–181. https://doi.org/10.1016/S0048-9697(01)00957-3.

Lei, X.T., Chen, M., Guo, L.D., Zhang, X.G., Jiang, Z.H., Chen, Z.G., 2019. Diurnal variations in the content and oxygen isotope composition of phosphate pools in a subtropical agriculture soil. Geoderma 337, 863–870. https://doi.org/10.1016/j.geoderma.2018.10.039.

Li, Q.M., Zhang, W., Wang, X.X., Zhou, Y.Y., Yang, H., Ji, G.L., 2007. Phosphorus in interstitial water induced by redox potential in sediment of Dianchi Lake, China. Pedosphere 17 (6), 739–746. https://doi.org/10.1016/S1002-0160(07)60089-7.

Li, W., Joshi, S.R., Hou, G., Burdige, D., Sparks, D.L., Jaisi, D.P., 2015. Characterizing phosphorus speciation of Chesapeake Bay sediments using chemical extraction, ^{31}P-NMR, and X-ray absorption fine structure spectroscopy. Environ. Sci. Technol. 49, 203–211. https://doi.org/10.1021/es504648d.

Liang, Y., Blake, R.E., 2006. Oxygen isotope signature of P_i regeneration from organic compounds by phosphomonoesterases and photooxidation. Geochem. Cosmochim. Acta 70, 3957–3969. https://doi.org/10.1016/j.gca.2006.04.036.

Liang, Y., Blake, R.E., 2009. Compound and enzyme-specific phosphodiester hydrolysis mechanisms revealed by δ^{18}O of dissolved inorganic phosphate: implications for marine P cycling. Geochem. Cosmochim. Acta 73, 3782–3794. https://doi.org/10.1016/j.gca.2009.01.038.

Liu, Y., Wang, J.F., Chen, J.A., Zhang, R.Y., Ji, Y.X., Jin, Z.X., 2019. Pretreatment method for the analysis of phosphate oxygen isotope (δ^{18}OP) of different phosphorus fractions in freshwater sediments. Sci. Total Environ. 685, 229–238. https://doi.org/10.1016/j.scitotenv.2019.05.238.

Mclaughlin, K., Silva, S., Kendall, C., Stuart-Williams, H., Paytan, A., 2004. A precise method for the analysis of δ^{18}O of dissolved inorganic phosphate in seawater. Limnol. Oceanogr-meth. 2, 202–212. https://doi.org/10.4319/lom.2004.2.202.

Murphy, J., Riley, J.P., 1962. A modified single solution method for the determination of phosphate in natural waters. Anal. Chim. Acta 26, 31–36. https://doi.org/10.1016/S0003-2670(00)88444-5.

Niu, X.Y., Wang, Y.H., Yang, H., Zheng, J.W., Zou, J., Xu, M.N., Wu, S.S., Xie, B., 2015. Effect of land use on soil erosion and nutrients in Dianchi Lake watershed, China. Pedosphere 25 (1), 103–111. https://doi.org/10.1016/S1002-0160(14)60080-1.

Pfahler, V., Dürr-Auster, T., Tamburini, F., Bernasconi, S.M., Frossard, E., 2013. ^{18}O enrichment in phosphorus pools extracted from soybean leaves. New Phytol. 197, 186–193. https://doi.org/10.1111/j.1469-8137.2012.04379.x.

Pistocchi, C., Tamburini, F., Gruau, G., Ferhi, A., Trevisan, D., Dorioz, J.-M., 2017. Tracing the sources and cycling of phosphorus in river sediments using oxygen isotopes: methodological adaptations and first results from a case study in France. Water Res. 111, 346–356. https://doi.org/10.1016/j.watres.2016.12.038.

Rutledge, J.M., Chow-Fraser, 2019. Landscape characteristics driving spatial variation in total phosphorus and sediment loading from sub-watersheds of the Nottawasaga River, Ontario. J. Environ. Manag. 234, 357–366. https://doi.org/10.1016/j.jenvman.2018.12.114.

Ruttenberg, K.C., 1992. Development of a sequential extraction method for different forms of phosphorus in marine sediments. Limnol. Oceanogr. 37 (7), 1460–1482. https://doi.org/10.4319/lo.1992.37.7.1460.

Sandy, E.H., Blake, R.E., Chang, S.J., Yao, J., Yu, Chan, 2013. Oxygen isotope signature of UV degradation of glyphosphate and phosphonoacetate: tracing sources and cycling of phosphonates. J. Hazard Mater. 260, 947–954. https://doi.org/10.1016/j.jhazmat.2013.06.057.

Song, X.Y., Ma, L., Zhao, H.X., Tu, Q., Lu, Y.F., Lu, S.Y., 2019. Purification effect and stability of water quality of different functional units in Laoyuhe Wetland Park of

Dianchi Lake (In Chinese). J. Environ. Eng. Technol. 9 (2), 167–174, 10.12153j.issn.1674-991X.2019.01.030.

Stout, L.M., Joshi, S.R., Kana, T.M., Jaisi, D.P., 2014. Microbial activities and phosphorus cycling: an application of oxygen isotope ratios in phosphate. Geochem. Cosmochim. Acta 138, 101–116. https://doi.org/10.1016/j.gca.2014.04.020.

Tang, X.Q., Wu, M., Li, R., 2018. Distribution, sedimentation, and bioavailability of particulate phosphorus in the mainstream of the Three Gorges Reservoir. Water Res. 140, 44–55. https://doi.org/10.1016/j.watres.2018.04.024.

Tian, L.Y., Guo, Q.J., Yu, G.R., Zhu, Y.G., Lang, Y.C., Wei, R.F., Hu, J., Yang, X.R., Ge, T. D., 2020. Phosphorus fractions and oxygen isotope composition of inorganic phosphate in typical agricultural soils. Chemosphere 239, 124622. https://doi.org/10.1016/j.chemosphere.2019.124622.

van Cappellen, P., Berner, R.A., 1991. Fluorapatite crystal growth from modified seawater solutions. Geochem. Cosmochim. Acta 55, 1219–1234. https://doi.org/10.1016/0016-7037(91)90302-l.

Wang, J., Huang, T., Wu, Q.Q., Bu, C.C., Yin, X.J., 2021. Sources and cycling of phosphorus in sediment of rivers along a eutrophic lake in China indicated by phosphate oxygen isotopes. ACS. Earth. Space. Chem. 5, 88–94. http://doi/10.1021/acsearthspacechem.0c00298.

Wang, J.F., Chen, J.A., Ding, S.M., Guo, J.Y., Christopher, D., Dai, Z.H., Yang, H.Q., 2016. Effects of seasonal hypoxia on the release of phosphorus from sediments in deep-water ecosystem: a case study in Hongfeng reservoir, Southwest China. Environ. Pollut. 219, 858–865. https://doi.org/10.1016/j.envpol.2016.08.013.

Wei, K., Zeng, X.W., Wang, C.S., Peng, Z.Q., Wang, J.P., Zhou, F.X., Chen, F.J., 2021. Phosphate distribution and sources in the waters of Huangbai River, China: using oxygen isotope composition of phosphate as a tracer. Environ. Sci. Pollut. Res. 28, 29732–29741. https://doi.org/10.1007/s11356-021-12808-x.

Wells, N.S., Gooddy, D.C., Reshid, M.Y., Williams, P.J., Smith, A.C., Eyre, B.D., 2022. $\delta^{18}O$ as a tracer of PO_4^{3-} losses from agricultural landscapes. J. Environ. Manage. 317, 11529. https://doi.org/10.1016/j.jenvman.2022.115299.

Wu, Z.H., Wang, S.R., 2017. Release mechanism and kinetic exchange for phosphorus (P) in lake sediment characterized by diffusive gradients in thin films (DGT). J. Hazard Mater. 331, 36–44. https://doi.org/10.1016/j.jhazmat.2017.02.024.

Xie, F.Z., Li, L., Song, K., Li, G.L., Wu, F.C., Giesy, J.P., 2019. Characterization of phosphorus forms in a eutrophic lake, China. Sci. Total Environ. 659, 1437–1447. https://doi.org/10.1016/j.scitotenv.2018.12.466.

Yuan, H.Z., Li, Q., Kukkadapu, R.K., Liu, E.F., Yu, J.H., Fang, H., Li, H., Jaisi, D.P., 2019. Identifying sources and cycling of phosphorus in the sediment of a shallow freshwater lake in China using phosphate oxygen isotopes. Sci. Total Environ. 676, 823–833. https://doi.org/10.1016/j.scitotenv.2019.04.322.

Zhao, M.Y., Blake, R.E., Liang, Y.H., Ruf, D.D., Jaisi, D.P., Chang, S.J., Planavsky, N.J., 2021. Oxygen isotopic fingerprints on the phosphorus cycle within the deep subseafloor biosphere. Geochem. Cosmochim. Acta 310, 169–186. https://doi.org/10.1016/j.gca.2021.05.018.

Zhu, Y.R., Wu, F.C., He, Z.Q., Guo, J.Y., Qu, X.X., Xie, F.Z., Giesy, J.P., Liao, H.Q., Guo, F., 2013. Characterization of organic phosphorus in lake sediments by sequential fractionation and enzymatic hydrolysis. Environ. Sci. Technol. 47, 7679–7687. https://doi.org/10.1021/es305277g.